Extreme Weather Events and Climate Extremes are Limited by the Duration of Solar Cycle Irradiance Extremes

Robert Weber[1]

[1]Self Employed

November 21, 2022

Abstract

Understanding the simple mechanism of variable solar irradiance ocean warming/cooling allows for effective attribution, detection, and prediction of ocean-related extreme weather events based on solar activity level and duration. Modern and historical solar and ocean data were used to find the ocean warms from rising and high solar activity over any duration, and vice-versa, such as cooling from low activity during the Dalton Minimum. Equatorial ocean heat content and sea surface temperature are sensitive to daily total solar irradiance (TSI) variation and level, and to the upwelled heat accumulation from prior days sub-surface absorbed solar energy penetration. Equatorial evaporation from the absorbed solar energy performs as the pump of Earth's hydrological system, sourcing atmospheric rivers and associated extreme weather events, follows a solar cycle pattern. Decadal scale ocean warming and post-solar cycle maximum El Nino events were empirically found to occur after solar activity rises above a decadal average of 120 sfu F10.7cm, equivalent to 94 v2 SIDC sunspot number and 1361.25 W/m2 LASP SORCE TSI. HadSST3 was found to linearly vary with the annual change in TSI, nominally at 0.5°C/W/year, varying with rate of TSI change. An empirical F10.7-TSI-SST model was derived combining a F10.7cm-SORCE TSI correlation model and the HadSST3-TSI sensitivity factor, predicated on the SWPC Solar Cycle 24 panel 2016 F10.7cm flux forecast. The author used this model in December of 2015 to uniquely and successfully predict the 2016 HadSST3 temperature fall to within 0.03°C. Cross correlation analysis indicate solar minimum La Nina events result from insufficient TSI over time, producing less equatorial evaporation, less cloud cover and precipitation, causing drought in the US. The Solar Modern Maximum that peaked in late 2003 warmed the ocean creating 20th century climate change via higher than average solar activity, higher than the 1361.25 W/m2 decadal TSI warming threshold. The 2003 European heat wave was forced by cumulative high solar activity warming of the AMO, and from high TSI during the heat wave. The 2013/14 Cold Wave is partly attributable to periods of lower than solar minimum level irradiance from October 2013 through February 2014. Future extremes depend on the duration of future solar cycle activity extremes.

Extreme Weather Events and Climate Extremes are Limited by the Duration of Solar Cycle Irradiance Extremes

AGU100 2018 Fall Meeting Poster Session
Climate Extremes: Patterns, Mechanisms, and Attribution
Abstract GC21E-1144

Robert Weber

Abstract

Understanding the simple mechanism of variable solar irradiance ocean warming/cooling allows for effective attribution, detection, and prediction of ocean-related extreme weather events based on solar activity level and duration. Modern and historical solar and ocean data were used to find the ocean warms from rising and high solar activity over any duration, and vice-versa, such as cooling from low activity during the Dalton Minimum. Equatorial ocean heat content and sea surface temperature are sensitive to daily total solar irradiance (TSI) variation and level, and to the upwelled heat accumulation from prior days sub-surface absorbed solar energy penetration. Equatorial evaporation from the absorbed solar energy performs as the pump of Earth's hydrological system, sourcing atmospheric rivers and associated extreme weather events, follows a solar cycle pattern.

Decadal scale ocean warming and post-solar cycle maximum El Nino events were empirically found to occur after solar activity rises above a decadal average of **120** sfu F10.7cm, equivalent to **94** v2 SIDC sunspot number and **1361.25** W/m² LASP SORCE TSI. HadSST3 was found to linearly vary with the annual change in TSI, nominally at **0.5** °C/W/year, varying with rate of TSI change. An empirical F10.7-TSI-SST model was derived combining a F10.7cm-SORCE TSI correlation model and the HadSST3-TSI sensitivity factor, predicated on the SWPC Solar Cycle 24 panel 2016 F10.7cm flux forecast. The author used this model in December of 2015 to uniquely and successfully predict the 2016 HadSST3 temperature fall to within **0.03** °C.

Cross correlation analysis indicate solar minimum La Nina events result from insufficient TSI over time, producing less equatorial evaporation, less cloud cover and precipitation, causing drought in the US. The Solar Modern Maximum that peaked in late 2003 warmed the ocean creating 20th century climate change via higher than average solar activity, higher than the **1361.25** W/m² decadal TSI warming threshold.

The 2003 European heat wave was forced by cumulative high solar activity warming of the AMO, and from high TSI during the heat wave. The 2013/14 Cold Wave is partly attributable to periods of lower than solar minimum level irradiance from October 2013 through February 2014. Future extremes depend on the duration of future solar cycle activity extremes.

Solar-Ocean Threshold Research & Development

Theory: Solar cycle 20 was too weak to warm the ocean, but SC21 wasn't - implying a 'breakeven' point, a solar energy 'threshold' for ocean warming.

Average daily solar activity for 2 periods of ***near-zero*** HadSST3 temperature anomaly ***change*** were calculated for sunspot number and F10.7cm flux.

Figure 1. Solar-Ocean Warming/Cooling *threshold*: *first estimated graphically*

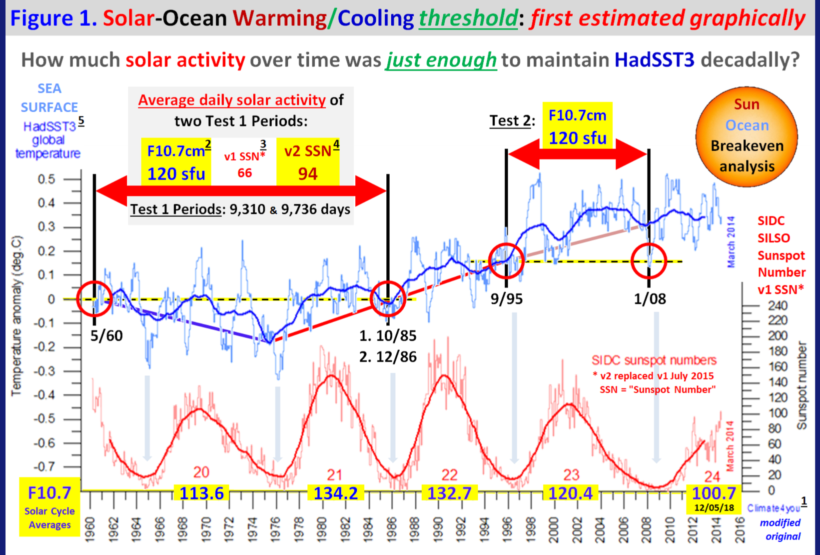

Table 1. Estimated Solar Indice Warming/Cooling Threshold Determinations

Test 1	Test 1 Periods		F10.7cm, sfu		SIDC v1 SSN		SIDC v2 SSN	
Start	5/1/1960	# days	sum	ave/day	sum	ave/day	sum	ave/day
End pt 1	10/31/1985	9,310	1,123,935	120.7	629,865	67.7	888,706	95.5
End pt 2	12/31/1986	9,736	1,155,503	118.7	635,764	65.3	895,122	91.9
Original Breakeven Calculations			ave	119.7	ave	66.5	ave	93.7
Nominal Solar Thresholds			F10.7cm	120	v1 SSN	66	v2 SSN	94

Two F10.7cm solar input models were tested with **120** sfu as a solar threshold coincident with decadal changes in HadSST3. Fig. 2 model defined "pauses".

Figure 2. Test 3: proxy solar input - F10.7cm running average since May 1, 1960

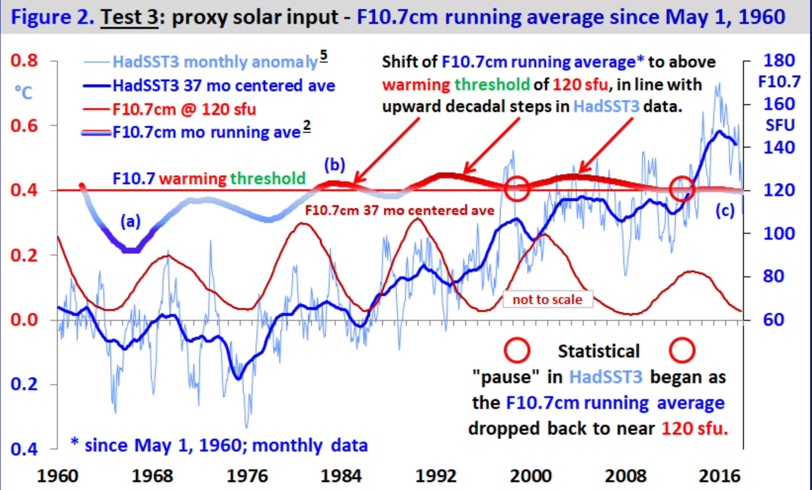

Accumulation model in fig.3 of sum of F10.7cm flux departure from 120 sfu peaked in YE 2003, matching HadSST3 peak; it fell below zero in Feb 2017.

Figure 3. Test 4: proxy solar input - Accumulated F10.7cm over/under 120 ±1 sfu

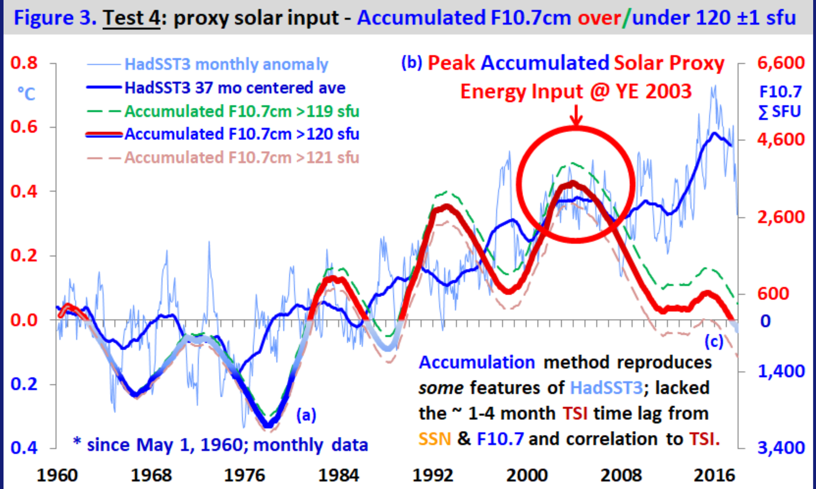

Total Solar Irradiance (TSI) Equivalent Threshold

Figure 4. TSI threshold: average of 2012 TSI & 3 models

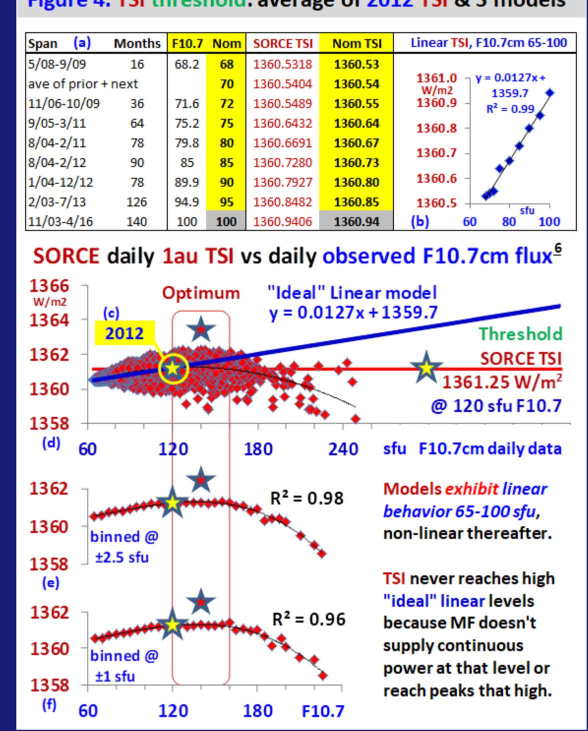

Span (a)	Months	F10.7	Nom	SORCE TSI	Nom TSI
5/08-9/09	16	68.2	68	1360.5318	1360.53
ave of prior + next			70	1360.5404	1360.54
11/06-10/09	36	71.6	72	1360.5489	1360.55
9/05-3/11	64	75.2	75	1360.6432	1360.64
8/04-2/11	78	79.8	80	1360.6691	1360.67
8/04-2/12	90	85	85	1360.7280	1360.73
1/04-12/12	78	89.9	90	1360.7927	1360.80
2/03-7/13	126	94.9	95	1360.8482	1360.85
11/03-4/16	140	100	100	1360.9406	1360.94

Figure 4 indicates LASP SORCE 1au TSI was correlated to DRAO F10.7cm flux in four ways to find a very close equivalent to **120** solar flux units.

The **2012** F10.7cm flux average was **119.7** sfu, average SORCE 1au TSI of **1361.24** W/m².

A yellow circle in fig. 4a-f shows the intersection of **2012 data** with a linear model and 2 binned models at **120** sfu F10.7cm & TSI of **1361.25** W/m², in panel (d), at a **±0.05** W/m² est. error.

Figure 5 below shows all the solar indices correlated together for 2003-2018, aligned and scaled to the 2007-09 solar minimum and solar-ocean threshold.

Figure 5. SIDC v2 SSN, DRAO F10.7cm, & LASP SORCE TSI ocean warming thresholds

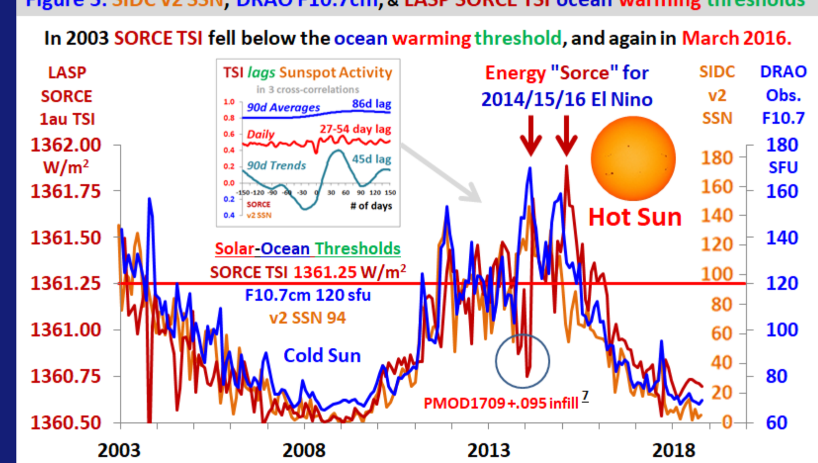

Cross-Correlation inset above, and fig. 6 below, indicate time-dependency of TSI on solar development, and the dependency of TSI on MF, respectively.

Figure 6. Comparing PMOD vs SORCE; PMOD by solar cycle vs |MF| and v2 SSN

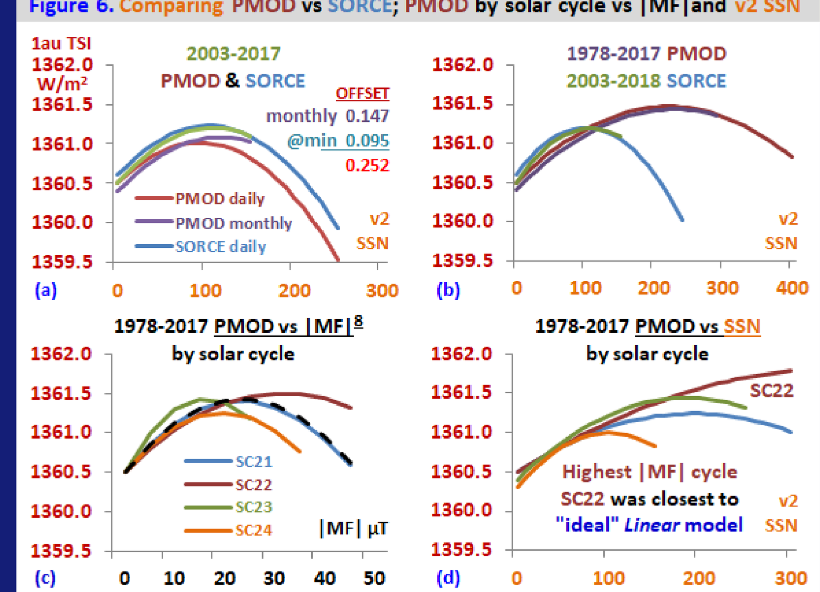

Figure 7a,b shows TSI is limited by solar magnetic mean field, limiting SST.

Figure 7. Solar Magnetic Field, MF, *limits* and *controls* TSI and HadSST3 changes

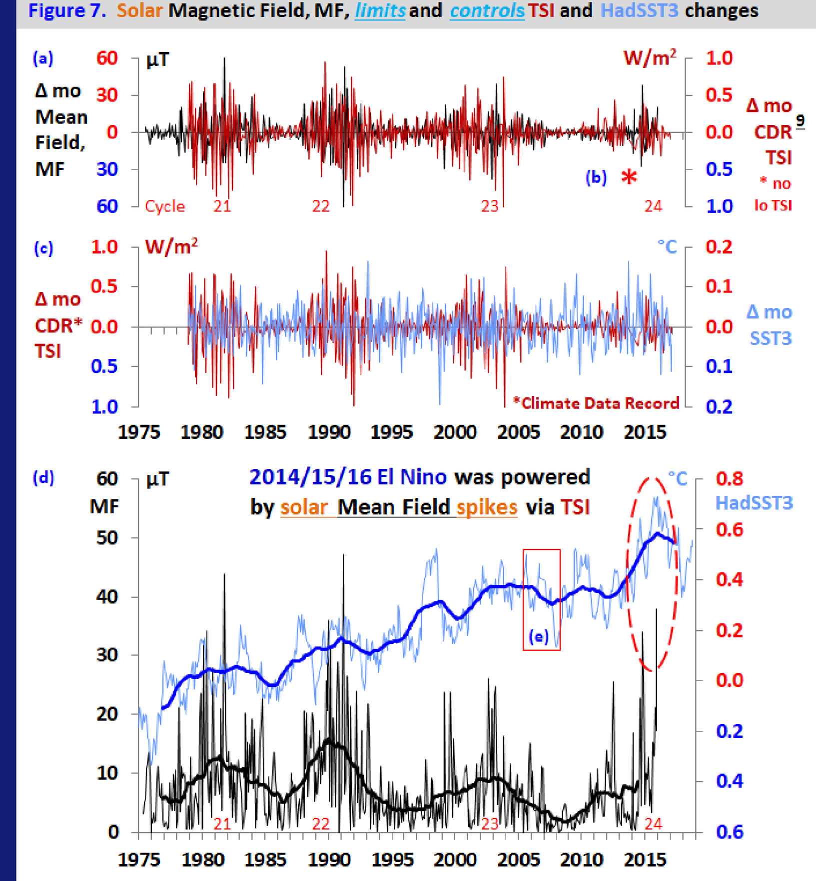

In fig. 7d, HadSST3 spikes are synced with solar mean field spikes. The red dashed oval shows the timing of the 2014/15 solar mean field spike(s) on the record El Nino. The fig. 7c red box is the training period for the empirically-derived HadSST3-TSI sensitivity factor, and was selected for the time of solar cycle, representative of previous solar cycle decline periods, but mainly as it was the only applicable time period during the short SORCE TSI record.

Figure 8. Stereo-A and SDO views of low to high activity range during solar cycle 24 from the minimum to the solar maximum, and back to solar minimum activity levels.[10]

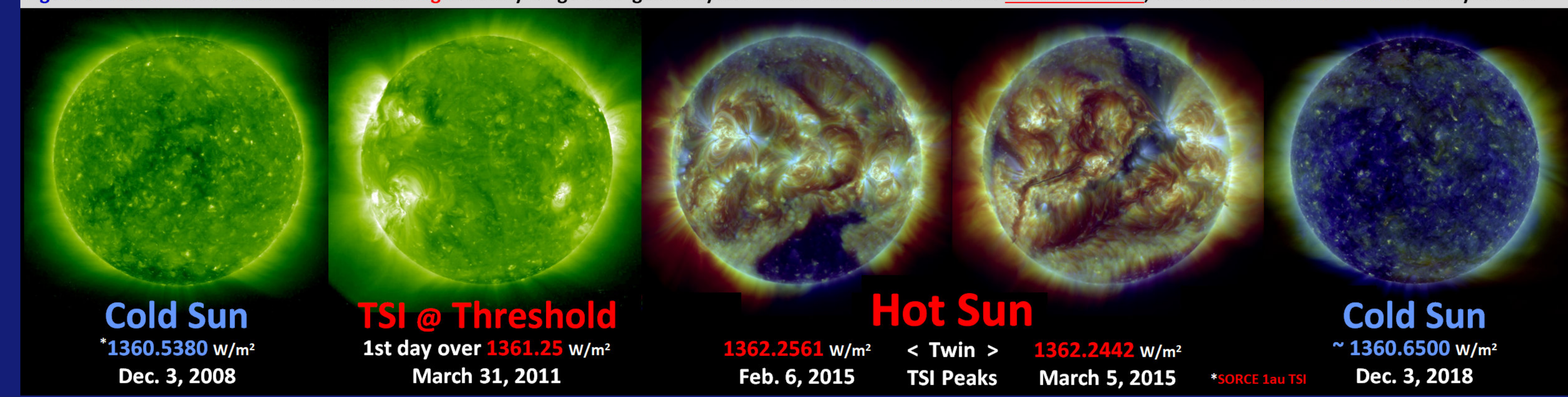

The Solar Cycle Influence: How TSI and Insolation Warm and Cool the Ocean

HadSST3-SORCE TSI Sensitivity Factor Calculated

Ocean surface temperature (HadSST3) declined during each of the solar cycle declining phases of the last six cycles, typified by cycle #23 in the red box in fig. 7, and below in the fig. 9 graph, (a), for 29 months. The sensitivity of HadSST3 to 1au TSI is calculated as the ratio of the change in ocean temperature to the change in 1au SORCE TSI, by two methods: (e) the fig. 7c red-boxed end-points that resulted in a nominal factor of **0.5** °C/W/year; and (f), the solar cycle 23 declining phase SST and TSI trends ratio is <**5**% of the fig. 9e red-boxed training period end-point calculated result.

Figure 9. HadSST3-SORCE TSI Sensitivity Factor Calculated

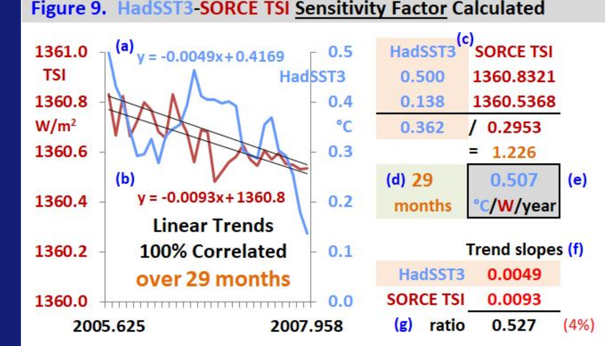

Solar-Ocean Supersensitivity & Climate Forecasting

In 2014, between the two red arrows in fig. 5, this author predicted in a blog[22] June 23, 2014 10:15am comment:

"Solar activity ramped up late last year and has since tapered off. The "recharge" of the oceans from that rampup is now dissipating. If and only if there is another spike in solar activity this year will there be an El Nino."
- Bob Weber *from* **"The 2014/15 El Niño – Part 11 – Is the El Niño Dying?"**

In late 2015, the author combined the F10.7cm-SORCE TSI correlation model from fig. 4b with the fig. 9e TSI-HadSST3 sensitivity factor, guided by the SWPC sunspot and radio flux prediction for the expected drop in 2016 solar activity, to forecast the 2016 HadSST3 ocean temperature change with the "best fit model" to the **0.03** °C HadSST3 uncertainty limit.

Table 2. The BEST FIT MODEL finds Dec 2016 HadSST3 within 0.03°C, 12.7% error @ uncertainty limit

Model ΔTSI = 0.0127*ΔF10.7 — Model ΔSST = 0.507*ΔTSI

Empirical 0.507	Actual F10.7cm	Modelled ΔTSI	Actual SORCE TSI	Model Error	YE Low F10.7cm	HadSST3 °C	Modelled ΔSST	Δ SST Error	Model Error
2015	117.8		1361.4321		112.5	0.592			
2016	88.8		1361.0073		81.2	0.613			bust
Δ	29	0.3683	0.4248	-13.3%	31.3	0.021	0.1867	0.2077	-88.8%
					SWPC				
Dec-15	112.5		1361.2527		Modelled	0.717	The BEST FIT MODEL		
Dec-16	75.3		1360.8154		ΔTSI	0.447	at uncertainty limit		
Δ	37.2	0.4724	0.4373	8.0%	0.3975	0.270	0.2395	0.030	12.7%
					-0.0335	20%			
	Ave of two:	0.4204	0.4310	-2.5%	-7.8%	0.64	0.2131	0.057	26.7%

YE 2016 HadSST3 @ 0.447°C was below 2014 @ 0.477°C, an impressive drop. HadSST3 uncertainty: 0.02-0.03°C

The cycle 24 sunspot maximum occurred in late 2014, followed by TSI twin peaks a solar rotation apart, lagging the sunspot peak. Fig.10a-f shows TSI sub-surface ocean warming, with equatorial ocean heat content (Eq OHC) increasing when TSI > **1361.25**, and vice versa. The OHC anomaly fell below zero as TSI < **1361.25**, confirming the author's 2014 solar-ocean threshold.

Figure 10. Solar Cycle 24 SORCE TSI peak powered Kelvin Waves and MJO via Equatorial OHC Accumulation

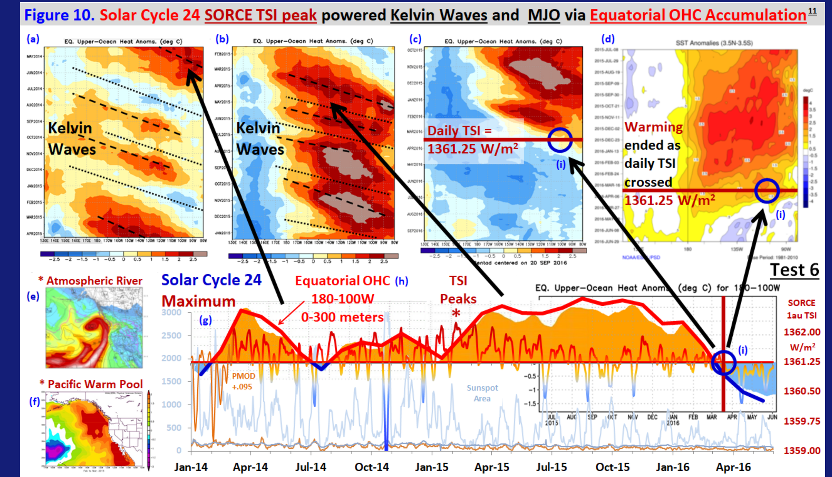

Statistically significant solar-climate correlations show solar cycle influence.

Figure 11. TSI vs Climate indices cross-correlations show Solar Cycle Influence on ENSO in 12yr window since 1979

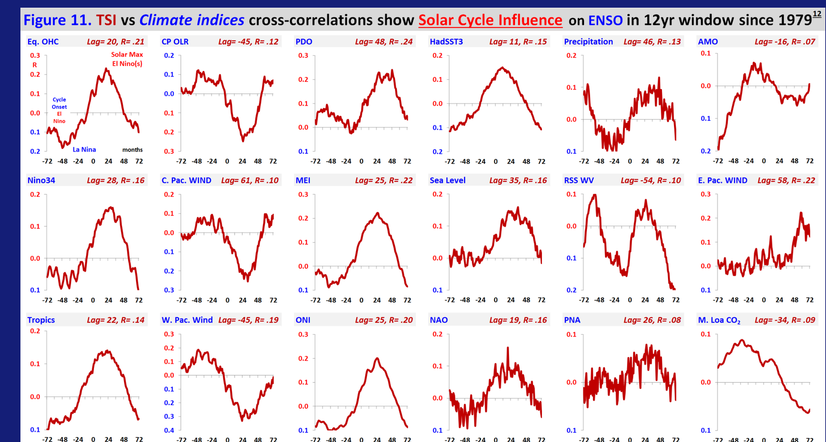

Figure 12. Ocean Temp. drives CO_2 outgassing & accumulation via Henry's Law[11]

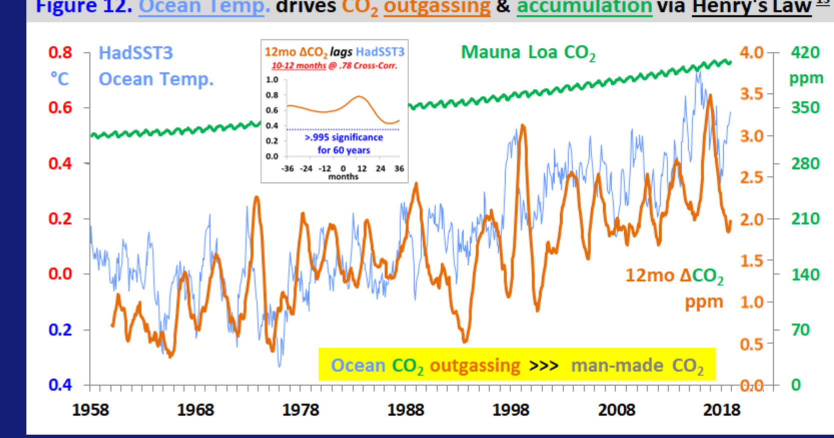

Atmospheric CO_2 accumulates from ocean outgassing during warming spikes.

Solar-Ocean Threshold defines Climate Changes

Figure 13. The Solar Cycle Influence on the Ocean

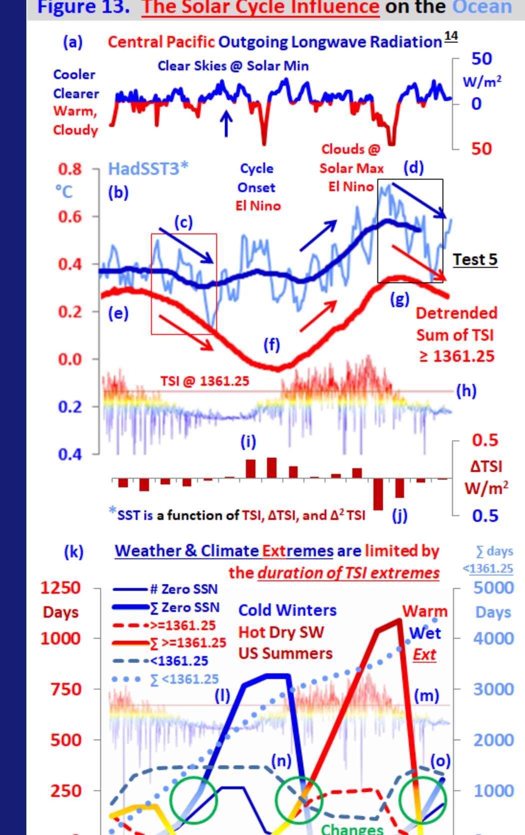

← Solar-ocean warming occurs in a generic solar cycle pattern starting with 'cycle onset El Nino' that is the Eq OHC reacting to the highest rate of annual TSI increase under solar minimum clear skies, then a La Nina until TSI rises above the threshold, when year-year ocean warming commences (fig. 13f-g).

Solar maximum El Nino(s) occurred after F10.7 had risen above **120** sfu, and TSI over **1361.25** W/m² for 2-3 years. The warming thresholds were first reached in solar cycle 24 in 2011, fig. 13f, n.

Long durations of zero sunspots and/or low TSI under **1361.25**W led to colder and snowier winters 2007-2010, and less summer rain in the SW US, leading to a deep drought increase that ended after warming began in 2011.

Future solar cycle 25 climate influence is estimated in fig. 14a-c, using former actual F10.7cm activity and projecting separately the old cycle's data forward from a common estimated starting date (a). The prior cycle models each have a long-term running average continuous with actual 2018 data(b), and an accumulation function, the detrended accumulated sum of F10.7 over/under **120** sfu [c], monthly data.

Figure 14. Solar Cycle 25 F10.7 *prior cycle models**

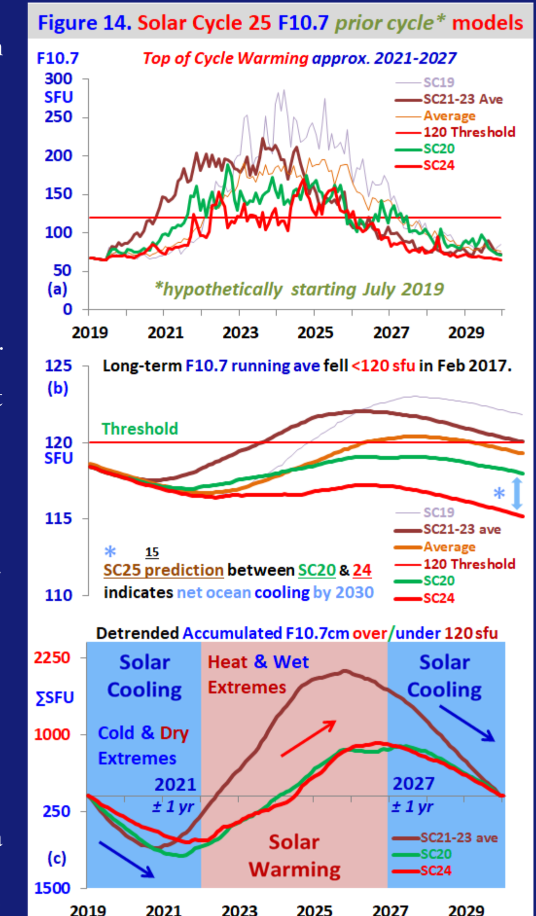

Cycle 25 sunspot activity of between cycles 20 & 24 would result in net ocean cooling by 2030; average activity will net small gain.

Figure 14c depicts the next cycle 25 as repeating the basic solar cycle generic warming/cooling pattern with a La Nina expected 2020-22, with increasing droughts from dry summer heat, followed by El Nino weather extremes after TSI has risen above the threshold through to the maximum, then cooling into the ~2030 solar min.

*LASP TSIS data replaces SORCE in cycle 25, with a new equivalent warming TSI threshold distinct to it, correlated to **120** F10.7cm.

Solar Activity Change creates Climate Change

HadSST3 in figs. 2, 3, 7d, and 12 depict the start of the great climate shift[23] in 1976, which started at the lowest point in solar-ocean heat accumulation since 1960. 1976 was also the start of solar cycle 21, which followed the generic solar-ocean forcing pattern(s) established in figs. 13,14.

Solar cycles 21-23 after 1976, together characterized in fig. 14 in the dark red high lines as an average, exhibited faster, stronger starts, and longer high sunspot activity above the ocean warming threshold, fig. 15f-h, due to the sun's strong magnetic mean field, fig. 15i.

Figure 15b-d, the equatorial ocean heat accumulation, the multi-variate ENSO index, and the central Pacific outgoing longwave radiation each followed a cycle-to-cycle repeating pattern driven by solar cycles activity changes that followed the generic solar-induced pattern introduced in figs. 13,14, indicating fundamental mechanisms repeating, as shown in the fig. 12 cross-correlations.

Long-term ocean warming since 1976 resulted from Eq OHC spreading out into the greater ocean when the solar activity for cycles 21-23 was higher than necessary for ocean warming, figs. 15f-i, driving HadSST3 upward, fig. 15c.

Figure 15. *Solar driven* >*1976 Climate Shift*: |MF| ave >6 µT warming line cycles 21-24*

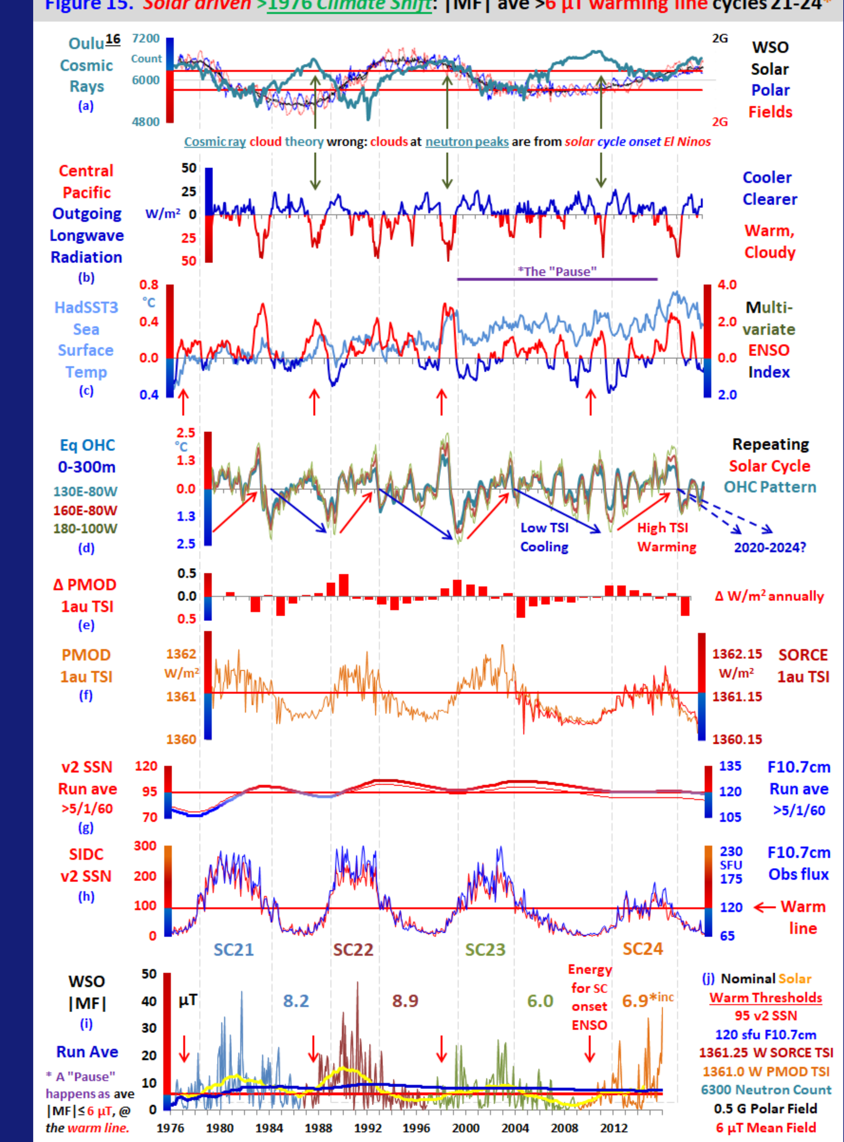

The solar modern maximum in sunspot activity, figure 16, was a 70-year long period when the average solar activity was higher than the previous 70 years, providing the power for climate changes since the Little Ice Age, figure 17.

Both figures illustrate the variety of solar activity regimes since 1818 & 1700.

Figure 16. The Sun's Modern Maximum in sunspot activity, from 1935-2004, warmed Earth via higher sunspot activity with far fewer cooling spotless days.

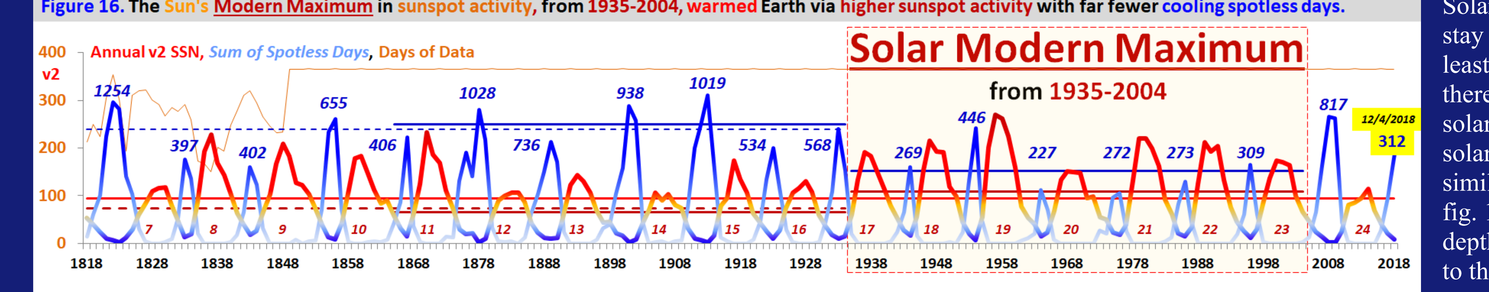

The Solar Modern Maximum compared to the prior record from 1818:

Sunspot numbers were *47% higher* during the 70 years from 1935-2004 than in the previous *117* years, 108.5 vs 73.8 annually from 1818-1934.

The intercycle average *sum of spotless days dropped 58%*, 721 to 299, and the annual average maximum # of spotless days fell from 240 to 152, -37%.

The Solar Modern Maximum compared to the previous equal time span:

Sunspot numbers were *65% higher* during the 70 years from 1935-2004 than in the previous *70* years, 108.5 vs 65.8 annually from 1865-1934.

The intercycle average *sum of spotless days dropped by 60%*, 746 to 299, and the annual average maximum # of spotless days fell from 250 to 152, -39%.

Figure 17. *Solar driven* >*1700s Climate Shift*: TSI-SST forcing evident over 300 years

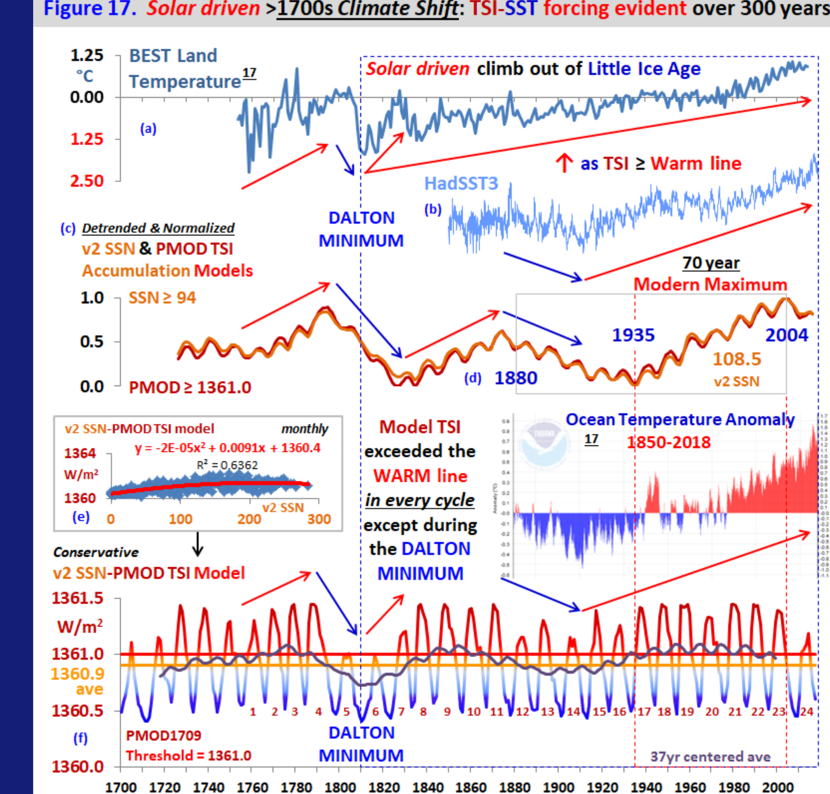

Solar Extremes Lead to Weather, Climate Extremes

Powerful solar irradiance above the decadal solar-ocean warming threshold during cycles 21-23 culminated during the summer of 2003 driving strong ocean warming driving a high AMO. **The sun's heat killed >70,000 people.**

Figure 18. 2003 European Heat Wave fueled by Modern Max high TSI, AMO[18]

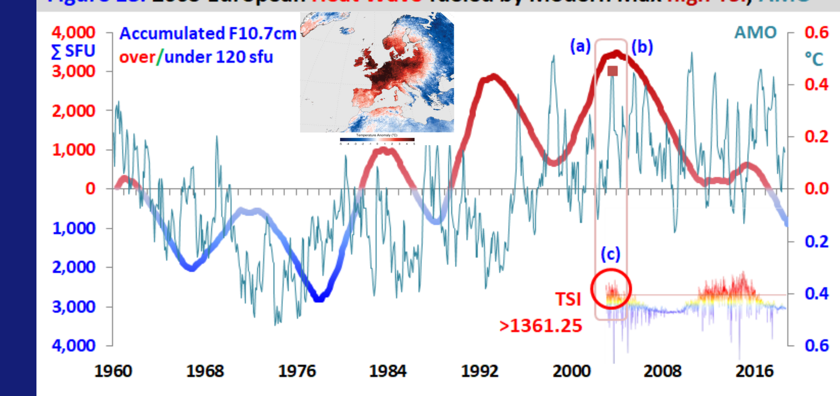

"The 2003 European heat wave led to the hottest summer on record in Europe since at least 1540.[1] Peer-reviewed analysis places the European death toll at more than 70,000.[2] The predominant heat was recorded in July and August, partly a result of the western European seasonal lag from the maritime influence of the Atlantic warm waters in combination with hot continental air and strong southerly winds." https://en.wikipedia.org/wiki/2003_European_heat_wave

Figure 19 below shows the 2013 fall/winter into early 2014 when very low TSI periods occurred because of the high sunspot areas driving a non-linear sunspot-TSI response, fig. 6, forcing several US cold waves (and elsewhere).

Figure 19. Record 2013/14 N. Hemisphere Winter Cold Wave *via low TSI*[19]

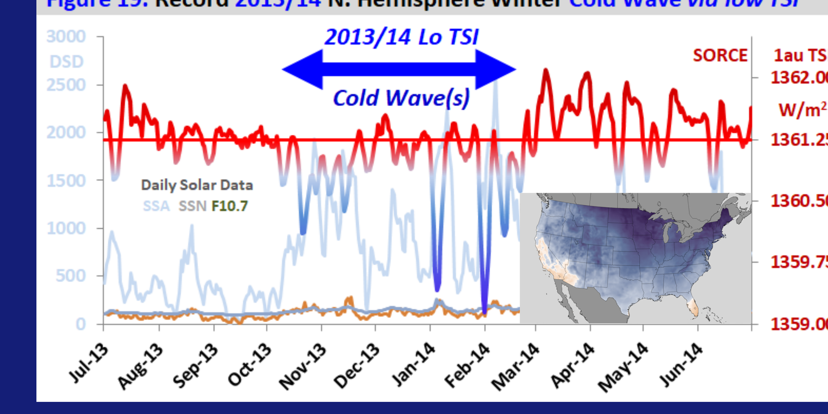

Under the long-term solar deficit of TSI energy under **1361.25** W/m², fig. 13k blue dotted line, the northern hemisphere is now cooling early each winter during the present solar minimum, in fig. 20, also evidenced by Greenland ice growth since early 2017, when the long-term F10.7cm running average since May 1960 fell below **120** sfu/day, meaning early hard winters until 2021± 1yr.

Figure 20. Record 2018 Cold Wave *via long duration low solar minimum TSI*

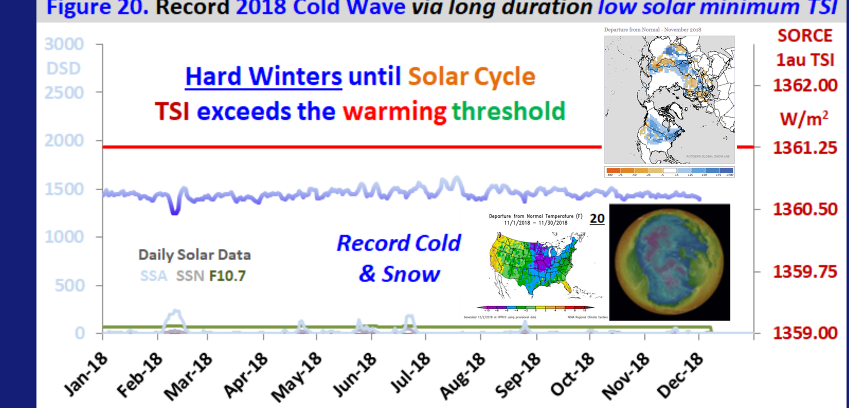

Earth has therefore dipped into a "mini-ice age" until TSI > Threshold.

Solar activity is predicted to stay in the low range for at least the next solar cycle. If there are two or more low solar cycles in a row the solar forcing trend will be similar to prior solar epochs, fig. 17c, with commensurate depth of cooling analogous to the Dalton Minimum.

Conversely a return to solar Modern Maximum levels of sunspot activity would lead to a long-term SST increase.

Conclusion

A new theory for a solar-ocean warming/cooling threshold based on solar activity levels and duration was investigated from 2014-2018, and it was found that the world ocean warms/cools over decadal solar cycle length periods when solar activity has reached sufficent strength, above the thresholds in fig. 15j.

This theory, now fully operational, replaces CO_2 and cosmic ray theories of warming/cooling, as CO_2 was found to be a consequence of TSI-warmed ocean outgassing, fig. 12, and clouds expected during low solar minimum activity when cosmic rays are high primarily originated from solar-warmed equatorial ocean during the solar cycle onset El Nino, fig. 15a.

TSI & insolation control the weather and climate.

Data Acknowledgements:
MET, NOAA, NASA, WSO, SIDC, LASP DRAO, RSS, SWPC, PMOD, UW, ESRL

The Sun causes warming, cooling, and extreme events, not CO_2.

Author conducted & funded research presented 12/11/18 in Washington, DC

Climate change is fundamentally reducible to daily TSI, not CO_2.

Bob Weber